Received: 1 September 2022 | Accepted: 22 October 2022

DOI: 10.1097/HC9.0000000000000018

ORIGINAL ARTICLE

OPEN

Prominin-1 promotes restitution of the murine extrahepatic biliary luminal epithelium following cholestatic liver injury

Allen Zhong[1] | **Celia Short**[1] | **Jiabo Xu**[1] | **G. Esteban Fernandez**[2] | **Nicolas Malkoff**[1] | **Nicolas Noriega**[1] | **Theresa Yeo**[1] | **Larry Wang**[3] | **Nirmala Mavila**[4] | **Kinji Asahina**[5] | **Kasper S. Wang**[1]

[1]Developmental Biology, Regenerative Medicine, and Stem Cell Program, The Saban Research Institute, Children's Hospital of Los Angeles, Los Angeles, California, USA

[2]Cellular Imaging Core, The Saban Research Institute, Children's Hospital of Los Angeles, Los Angeles, California, USA

[3]Department of Pathology, Children's Hospital Los Angeles, Los Angeles, California, USA

[4]Department of Medicine, Cedars Sinai Medical Center, Los Angeles, California, USA

[5]Central Research Laboratory, Shiga University of Medical Science, Ōtsu, Shiga Prefecture, Japan

Correspondence
Kasper S. Wang, MD, FACS, FAAP The Hospital for Sick Children 555 University Avenue, 1526 Hill Wing, Toronto, Ontario, Canada M5G 1X8
Email: kasper.wang@sickkids.ca

Funding information
Supported by U01 DK084538 (K.S.W.) and JSPS KAKENHI 22H02655 (K.A.).

Abstract

Background and Aims: Restitution of the extrahepatic biliary luminal epithelium in cholangiopathies is poorly understood. Prominin-1 (Prom1) is a key component of epithelial ciliary body of stem/progenitor cells. Given that intrahepatic Prom1-expressing progenitor cells undergo cholangiocyte differentiation, we hypothesized that Prom1 may promote restitution of the extrahepatic bile duct (EHBD) epithelium following injury.

Approach and Results: Utilizing various murine biliary injury models, we identified *Prom1*-expressing cells in the peribiliary glands of the EHBD. These *Prom1*-expressing cells are progenitor cells which give rise to cholangiocytes as part of the normal maintenance of the EHBD epithelium. Following injury, these cells proliferate significantly more rapidly to repopulate the biliary luminal epithelium. Null mutation of *Prom1* leads to significantly >10-fold dilated peribiliary glands following rhesus rotavirus–mediated biliary injury. Cultured organoids derived from *Prom1* knockout mice are comprised of biliary progenitor cells with altered apical-basal cellular polarity, significantly fewer and shorter cilia, and decreased organoid proliferation dynamics consistent with impaired cell motility.

Conclusions: We, therefore, conclude that Prom1 is involved in biliary

Abbreviations: BALB/c, Bagg albino/c; BDL, bile duct ligation; DDC, 3,5-diethoxycarbonyl-1,4-dihydrocollidine; DOL, day of life; EHBD, extrahepatic bile duct; FERM, 4.1, Ezrin, Radixin, Moesin; GFP, green fluorescent protein; KRT19, keratin 19; PBG, peribiliary gland; PDX1, pancreatic and duodenal homeobox 1; Prom1, Prominin-1; RRV, rhesus rotavirus; SOX17, sex-determining region Y-box 17; SOX9, sex-determining region Y-box 9.

Supplemental Digital Content is available for this article. Direct URL citations appear in the printed text and are provided in the HTML and PDF versions of this article on the journal's website, www.hepcommjournal.com.

epithelial restitution following biliary injury in part through its role in supporting cell polarity.

INTRODUCTION

Bile flows through the liver via a network of branching intrahepatic ducts that converges toward the extrahepatic bile duct (EHBD), which then drains bile into the gastrointestinal tract to support digestion and absorption of nutrients and vitamins. Various diseases, such as primary sclerosing cholangitis and biliary atresia (BA), are associated with obstruction of the EHBD ultimately causing intrahepatic cholestasis, fibrosis, and liver failure. BA is the leading cause of pediatric end-stage liver disease.[1,2] The processes by which EHBD is damaged and repairs itself are poorly understood.

We have previously reported that intrahepatic expression of transmembrane glycoprotein Prominin-1 (Prom1, aka CD133) is upregulated in infants with BA and in the murine model of BA based on rhesus rotavirus (RRV) infection.[3] Prom1 is strongly expressed by a population of periportal hepatic progenitor cells that proliferate following cholestatic injury and differentiate towards cholangiocytes comprising intrahepatic biliary ductular reactions.[4–6] Complete loss of function via null mutation of *Prom1* is associated with a reduction in ductular reactions and decreased intrahepatic fibrosis in RRV-mediated injury.[3,4]

The function of Prom1 is an area of active investigation.[7] Prom1 has been linked in both tumorigenesis through cancer stem cell proliferation [7,8] as well as epithelial progenitor cell proliferation and differentiation.[9–13] Prom1 has been implicated in cytoskeletal formation and remodeling, specifically via establishing apical microvilli and regulating ciliary structure and function.[14] Prom1 has also been shown to directly interact with the cytoskeletal FERM (*4*.1 protein, *E*zrin, *R*adixin, *M*oesin) family of proteins.[15] Recent genomic analyses demonstrate an association of cholangiopathies including BA with genetic polymorphisms involving both the structure and function of the cytoskeleton and cilia.[16]

The EHBD is a luminal structure consisting of a single layer of biliary epithelium surrounded by connective tissue containing blood vessels, lymphatics, smooth muscle, and nerves. Glandular structures, known as peribiliary glands (PBGs), reside within the EHBD wall contiguous with the main lumen. PBGs are comprised of biliary epithelial progenitor cells that proliferate and give rise to cholangiocyte progeny in response to biliary injury.[17] These PBG cells express both progenitor cell markers, such as sex-determining region Y-box (SOX)-9, SOX17, and pancreatic and duodenal homeobox 1 (PDX1), as well as mature cholangiocyte surface proteins involved in biliary solute transport.[17,18]

Herein, we hypothesize that Prom1-expressing progenitor cells residing in PBGs are involved in biliary epithelial restitution following cholestatic liver injury. Using several cholestatic liver injury models in mice, we observe that Prom1 plays a significant role in re-populating the EHBD lumen and that null mutation leads to significant morphologic changes and *in vitro* organoid behavior suggestive of a ciliopathy.

MATERIALS AND METHODS

Transgenic mouse model

Prom1$^{CreERT2\text{-}nLacZ}$ (*Prom1*^{Cre}) transgenic mice in C57BL/6N background (Jackson Laboratory), with a Cre recombinase and nuclear β-galactosidase (LacZ) cassette knocked-into the *Prom1* gene locus, were backcrossed into a Bagg albino/c (BALB/c) background over at least 7 generations (Charles River Laboratories). *Rosa26*$^{Lsl\text{-}GFP}$ (*GFP*) and *Rosa26*$^{tm4(ACTB\text{-}mTmG)}$ (*mTmG*) were bred in for reporter genes as described.[7,19] *Prom1*$^{Cre/+}$-*GFP*$^{+/-}$ and *Prom1*$^{Cre/+}$-*mTmG*$^{+/-}$ mice were generated for lineage tracing experiments, and injected then with tamoxifen (Sigma; 0.25 mg/g body weight) before injury model protocols. All experiments were performed in accordance with a protocol approved by the Institutional Animal Care and Use Committee (IACUC) of Children's Hospital Los Angeles.

Cholestatic biliary injury model

Adult *Prom1*$^{Cre/+}$-*GFP*$^{+/-}$ mice (>6 weeks of age) were injected with tamoxifen 0.25 mg/g body weight intraperitoneally. They were then placed on a control standard chow diet or a 0.1% grain-based 3,5-diethoxycarbonyl-1,4-dihydrocollidine (DDC) (Bio-Serv) diet 1 week after tamoxifen injection as previous described.[18] DDC was continued for 2 weeks and then transitioned to a standard chow diet. Fresh EHBD tissue were collected from both control and DDC diet groups up to and 6 weeks after diet initiation.

Adult *Prom1*$^{Cre/+}$-*GFP*$^{+/-}$ mice were injected with tamoxifen intraperitoneally. Mice underwent bile duct ligation (BDL) surgery as described.[4] In brief, mice were anesthetized with sevoflurane and then prepped sterilely. At laparotomy, the EHBD was then dissected free and ligated with a silk suture distally. The abdomen was then closed in 2 layers. Postoperatively, mice were carefully monitored. Fresh EHBD tissue were collected at 4 and 21 days after surgery.

Prom1$^{Cre/+}$-*GFP*$^{+/-}$ and *Prom1*$^{Cre/Cre}$ (functionally *Prom1* knockout, herein *Prom1*^{KO}) -*GFP*$^{+/-}$ newborn pups with a BALB/c background were injected with tamoxifen at 0.25 mg/g at day of life (DOL) 0 and inoculated intraperitoneally with 1.5×10^6 colony forming units RRV (or saline) on DOL3 to induce experimental BA as described.[20] EHBD were collected for histologic analysis up to 18 days after injection.

For all animal procedures, both male and female mice were utilized and evenly distributed between experimental arms. Animals were euthanized via CO_2 asphyxiation and cervical dislocation at time of sample collection in accordance with IACUC protocols.

Human tissue samples

Proximal and distal human biliary remnant samples collected and stored on site in accordance with the Childhood Liver Disease Research Network protocol, "A Prospective Database of Infants With Cholestasis" (NCT00061828). Patient consent were obtained following approval from the Institutional Review Board (CCI-10-00148).

Live organoid imaging

Time-lapse images were obtained at intervals of 30 minutes with an Axio Observer 7 microscope equipped with a 2.5×/0.075 EC Plan-NEOFLUAR lens (Carl Zeiss Microscopy) and ORCA-Flash 4.0 LT+ camera (Hamamatsu Corp.). The voxel size was $2.6\times2.6\times200$ μm and the total Z-stack thickness was 1.6 mm (9 slices). The microscope stage was maintained at 37°C and supplied with prewarmed humidified ambient air mixed to 5% CO_2. The growth medium was manually exchanged for fresh medium in between time points every 3 days. The entire system was controlled with ZEN 2.6 blue. Images of extended depth of focus were created from the Z-stacks using the Wavelets method (ZEN), then misalignments due to media changes were corrected by aligning the time points with the Linear Stack Alignment with SIFT plugin of FIJI ImageJ. Images were auto-scaled and converted to 8-bit before alignment.

Video reconstructions were then imported to FIJI ImageJ and segmented using a variance filter at a radius of 5 pixels and fill hole binary function. Frames were then manually edited to complete organoid segmentation and remove artifact. Segmented frames were then imported into Arivis Vision4D. Segments were then tracked through frames utilizing the track finder function. Data in the form of annotations were then exported.

For each experiment and organoid culture, the raw time series of organoid surface area was plotted over frame (time) data in Stata 15.1 (StataCorp), in addition to an XYZ-frame moving average. If the organoid size dropped below 20% of the moving average, this was counted as a "dip." Size oscillations were then characterized as surface area depressions $>50\%$ of the normalized surface area. Size oscillations were further defined as having to sustain a relative surface area depression to the normalized surface area function over at least 2 continuous time points (1 hour). We also verified these dips using a manual counting measure; the concordance of both measures had a correlation of XYZ.

Statistical analysis

Statistics were performed with Graphpad Prism, Version 9 (Dotmatics). Where appropriate paired or unpaired *t* test and analysis of variance with post hoc Tukey and Mann-Whitney tests were performed. A $p < 0.05$ was considered statistically significant.

RNAscope, immunofluorescence staining, immunohistochemistry, organoid culture, fixation and staining, confocal microscopy and RNA-sequencing

Please see Supplemental Methods and Supplemental Tables 1 & 2. The data discussed in this publication have been deposited in NCBI's Gene Expression Omnibus (Zhong et al., 2022) and are accessible through GEO Series accession number GSE220054 https://www.ncbi.nlm.nih.gov/geo/query/acc.cgi?acc=GSE220054

RESULTS

PROM1 is expressed in the PBGs

We first observed that in the uninjured EHBD, PROM1 expression is most heavily expressed in KRT19$^+$ surface epithelial cells along the distal EHBD with little to no expression in the gallbladder in adult mice (Figure 1A). Within the distal EHBD, PROM1 is expressed predominantly in PBGs but not in the EHBD lumen. This was further validated by mRNA *in situ* hybridization with the observation of co-expression of *Prom1* with *Krt19* in PBG (Figure 1B). We further observed PROM1 strongly co-expressed with KRT19, SOX9, SOX17, and PDX1, all progenitor cell markers known to be expressed in PBGs (Figure 1C).[17]

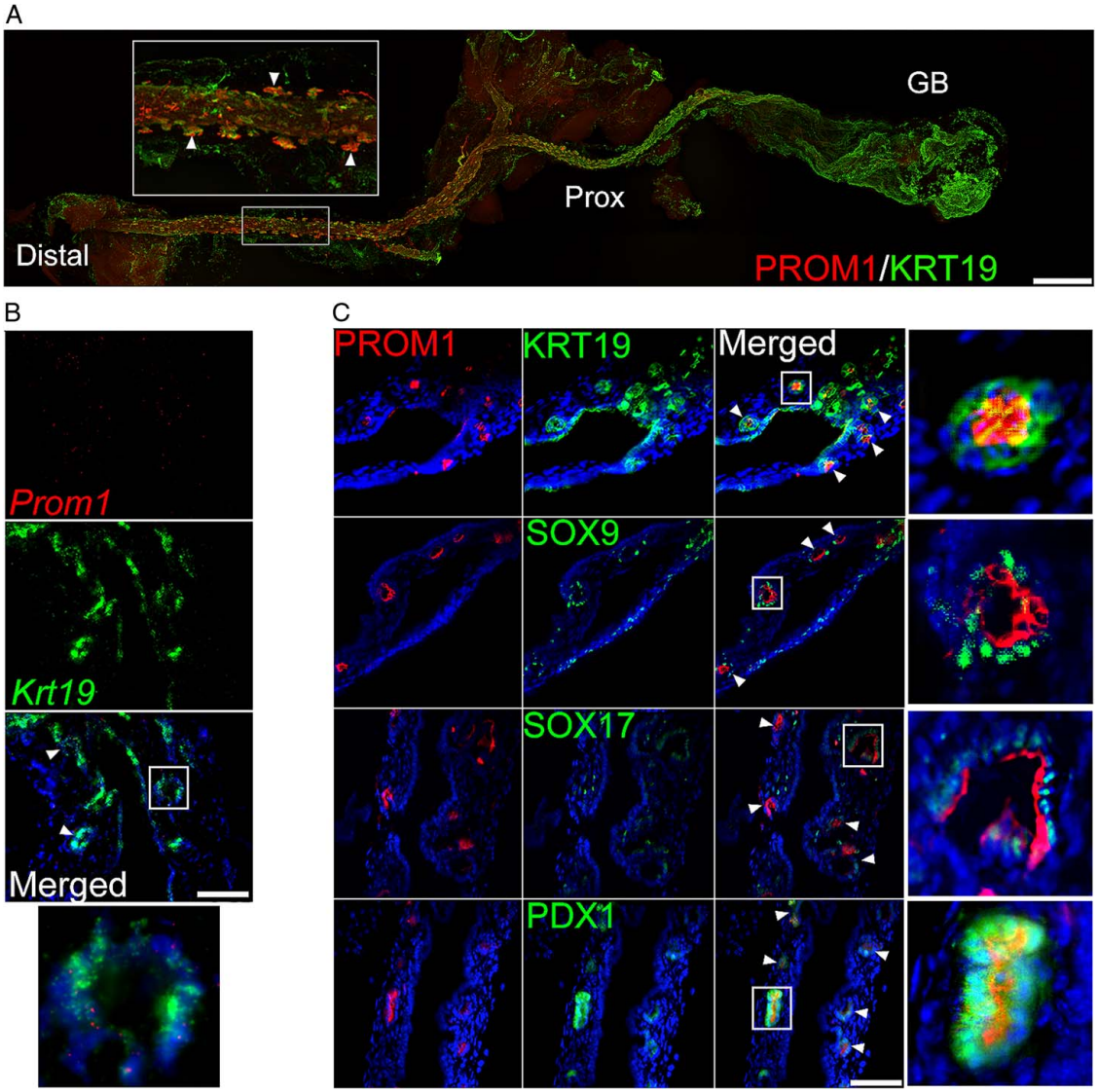

FIGURE 1 PROM1 expression in the PBGs of murine EHBD. (A) Whole mount imaging of PROM1 (red) and KRT19 (green) of a cleared adult EHBD. PROM1 expression is seen in the EHBD PBGs. Triangles point to PBGs. Scale bar, 100 μm. (B) RNA *in situ* hybridization demonstrates *Prom1* (red) and *Krt19* (green) co-expression PBGs. White box indicates zoomed-in insets. Nuclei were counterstained with DAPI. Scale bar, 50 μm. (C) PROM1 is co-expressed in PBGs with biliary progenitor cell markers SOX9, SOX17, and PDX1 (green). White boxes indicate zoomed-in insets of PBGs. Scale bar, 50 μm. Abbreviations: EHBD, extrahepatic bile duct; PBG, peribiliary gland; PDX1, pancreatic and duodenal homeobox 1; PROM1, Prominin-1; SOX9, sex-determining region Y-box 9; SOX17, sex-determining region Y-box 17.

Prom1-expressing progenitor cell lineage is involved in biliary epithelium maintenance and restitution following injury

To determine whether Prom1-expressing cells in PBGs act as biliary progenitor cells for the epithelium of the EHBD, we performed cell lineage tracing experiments to determine the fate of *Prom1*-expressing cells. Adult *Prom1*$^{Cre/+}$-*GFP*$^{+/-}$ mice were injected with tamoxifen 1 week before tissue collection (Figure 2A). At baseline, GFP is nearly exclusively expressed by PBG cells. After 6 weeks of control diet, we observed increasingly more GFP expression in the KRT19^{+} surface epithelium (Figure 2B, C). This observation suggests that Prom1-expressing biliary progenitors are involved in biliary epithelial maintenance.

We then sought to determine if *Prom1*-expressing biliary progenitors are involved in biliary epithelial restitution following injury. Adult mice were fed with a DDC diet for 2 weeks to induce biliary injury via chemical cholangiocyte oxidative toxicity. Mice were then switched back to a regular chow diet after 2 and 4 weeks of DDC diet period to establish a period of recovery (Figure 2A).[21] We observed more GFP expression in the surface biliary epithelium following DDC injury compared with control. The fraction of GFP-

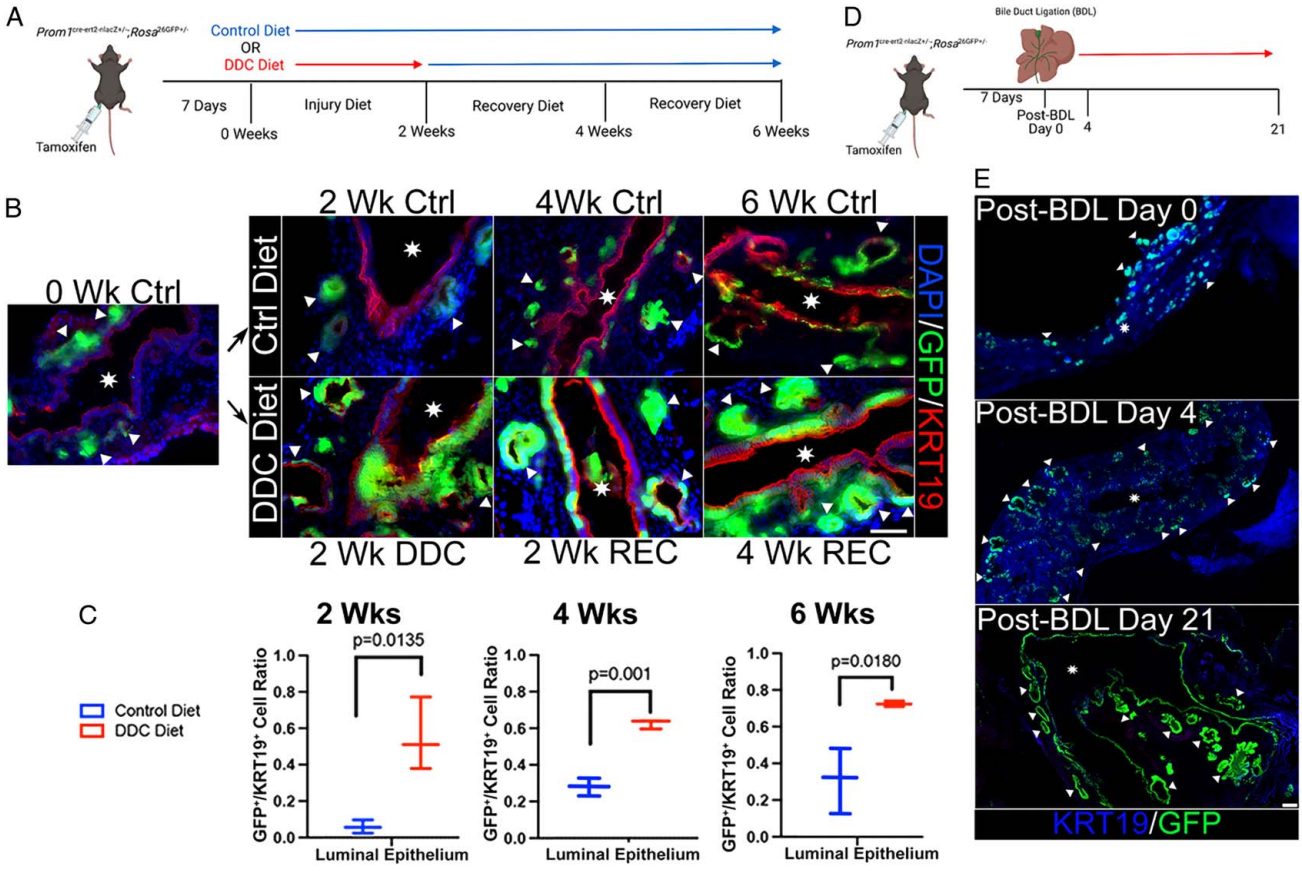

FIGURE 2 *Prom1*-expressing biliary progenitor cells residing in PBGs and their lineage re-populate the EHBD surface epithelium after injury in adult mice. (A) *Prom1*$^{Cre/+}$-*GFP*$^{+/-}$ mice were injected with tamoxifen 1 week before DDC or standard chow control diet initiation. EHBDs were then collected at 0, 2, 4, and 6 weeks. (B) Fluorescence imaging of EHBDs from mice fed control or DDC diet. GFP (green), and thus *Prom1*-expressing cells and their lineage are confined to PBGs in early control diet. GFP is seen in the surface epithelium in DDC. Triangles point to PBGs. Stars signify EHBD lumen. Scale bar, 50 μm. (C) The proportion of surface epithelial PROM1 lineage (GFP$^+$/KRT19$^+$ double positive) per high-power field is higher in DDC groups compared with their respective control diet group (n = 3 biological replicates at each time point). (D) *Prom1*$^{Cre/+}$-*GFP*$^{+/-}$ mice injected with tamoxifen 1 week before bile duct ligation (BDL) surgery. EHBD were collected at post-BDL day s0, 4, and 21. (E) Whole mount microscopy of EHBDs after BDL surgery. GFP is confined to PBGs without surgery (top panel), but small amounts of surface GFP is expressed in early injury (middle panel, post-BDL day 4). Surface epithelium nearly universally GFP$^+$ in late injury (bottom panel, post-BDL day 21). Scale bar, 200 μm. Abbreviations: BDL, bile duct ligation; Ctrl, control; DDC, 3,5-diethoxycarbonyl-1,4-dihydrocollidine; EHBD, extrahepatic bile duct; GFP, green fluorescent protein; PBG, peribiliary gland; *Prom1*, Prominin-1; REC, recovery; Wk, week. Images are high-resolution stills from Supplemental Videos 1 (http://links.lww.com/HC9/A40) and 2 (http://links.lww.com/HC9/A41).

positive cells then increased over time after DDC diet was removed and was statistically more than the control diet at all time points (Figure 2B, C).

We observed a similar pattern of biliary epithelial restitution following distal BDL (Figure 2D). As seen above, GFP is limited to the PBGs early on without injury in *Prom1*$^{Cre/+}$-*GFP*$^{+/-}$ mice (Figure 2E and Supplemental Video 1). Four days after BDL surgery, GFP expression is present in a few rare surface epithelial cells (Figure 2E); however, by 21 days after BDL surgery, nearly all the surface epithelium expresses GFP (Figure 2E and Supplemental Video 2). GFP-expressing PBGs appear to dilate during the observation period, which supports the possibility that PROM1-expressing biliary progenitor cells are giving rise to GFP-expressing daughter cells in an increasingly crowded niche.

Prom1-expressing progenitor cell lineage is involved in EHBD luminal growth and restitution following neonatal injury

To determine if a similar pattern of biliary epithelial maintenance/restitution is employed in the neonatal period, we utilized a modified murine model of BA, where newborn mouse pups are injected with RRV or saline at DOL3 (Figure 3A) to induce an infectious and autoimmune-mediated injury to the biliary epithelium. In contrast to DOL0 RRV injections, DOL3 injections are not associated with complete EHBD obliteration and therefore longer survival for observation.[22] Neonatal *Prom1*$^{Cre/+}$-*GFP*$^{+/-}$ from a BALB/c background were intraperitoneally injected with tamoxifen at DOL0. In control pups, we observed a similar pattern, as in adult mice, of GFP expression exclusively by PBG cells with

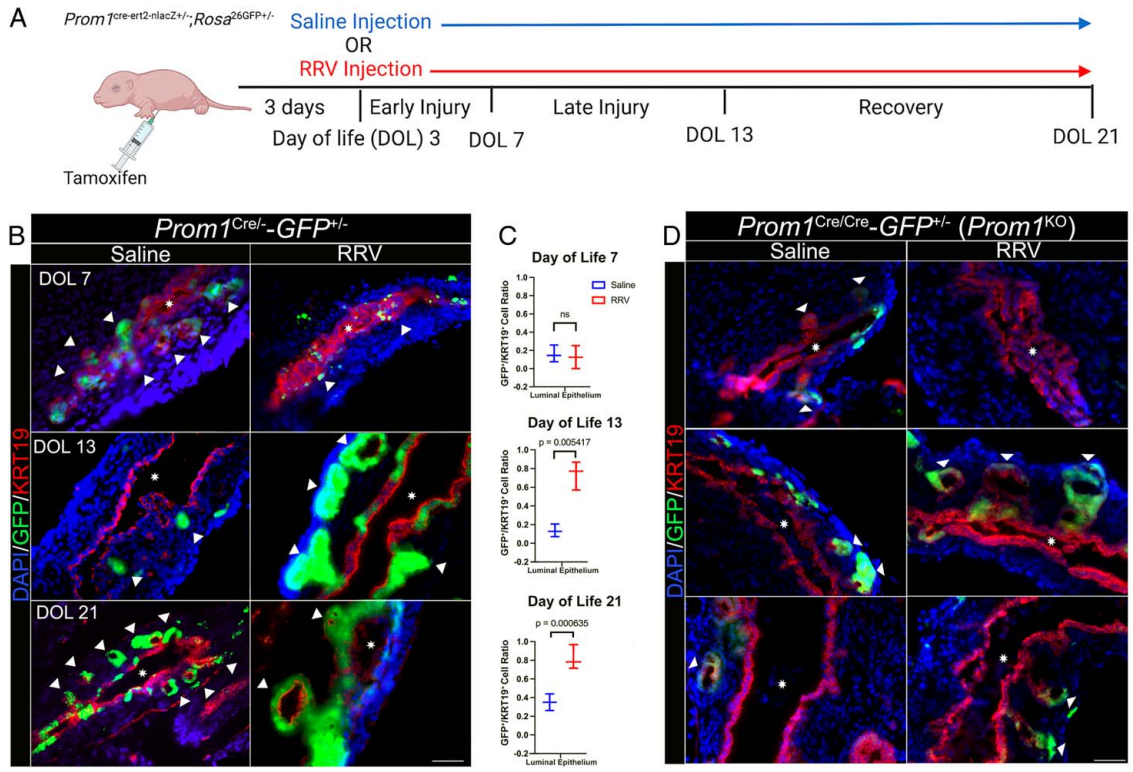

FIGURE 3 *Prom1*-expressing biliary progenitor cells and their lineage re-populate the EHBD surface epithelium after the murine BA model of RRV injection. (A) *Prom1*$^{Cre/+}$-*GFP*$^{+/-}$ mice from a BALB/c background were injected with tamoxifen on DOL0. Saline or RRV injection were performed on DOL3. EHBDs were collected at DOL7, DOL13, and DOL21. (B) GFP is limited to the PBGs in the saline group. Surface epithelial GFP expression increases in RRV as time from injury progresses. Scale bar, 50 μm. (C) Surface GFP expression is statistically higher in RRV injured versus saline control at all time points except postinjection day 4 (n = 3 biological replicates at each time point). (D) RRV injury was replicated in *Prom1*$^{Cre/Cre}$-*GFP*$^{+/-}$ (*Prom1*^{KO}) mice. GFP is limited to the PBGs in both saline and injury groups. Surface epithelial GFP expression is limited in the luminal epithelium as time from injury progresses in the RRV group. Scale bar, 50 μm. Abbreviations: BA, biliary atresia; EHBD, extrahepatic bile duct; GFP, green fluorescent protein; PBG, peribiliary gland; *Prom1*, Prominin-1; RRV, rhesus rotavirus.

increasing GFP positivity along the surface biliary epithelium over time (Figure 3B). Injury with RRV injection was associated with much greater GFP positivity compared with controls in the surface biliary epithelium at 10 days postinjection and beyond (Figure 3C).

The RRV injury model was then replicated in neonatal *Prom1*$^{Cre/Cre}$-*GFP*$^{+/-}$ (functional *Prom1*^{KO}) transgenic mice. Notably, GFP positivity, even in RRV injury state through DOL21 remained primarily within the PBG with minimal GFP expression the luminal epithelium after injury compared with the *Prom1*$^{Cre/+}$-*GFP*$^{+/-}$ (*Prom1*-expressing) transgenic EHBD (Figure 3D).

To further characterize the role of Prom1 in biliary epithelial restitution, neonatal wild-type (*Prom1*^{WT}) and *Prom1* knockout (*Prom1*^{KO}) mice in a BALB/c background were injected with RRV at DOL3. EHBDs were then collected for comparison 18 days after injection. Interestingly, *Prom1*^{KO} PBGs were significantly larger than *Prom1*^{WT} at 18 days after RRV injection (Figure 4A). *Prom1*^{KO} PBGs were >10 times larger than those of *Prom1*^{WT} after injury (1484.4 ± 1156 vs. 126.1 ± 86.3 μm^2) (Figure 4B). This change in PBG architecture with null mutation of *Prom1* suggests a functional role for PROM1 in biliary progenitor cells during cholestatic injury in biliary epithelium. Hematoxylin and eosin staining of EHBD demonstrates dilation of *Prom1*^{KO} PBGs after RRV injury as compared with *Prom1*^{WT} PBGs (Figure 4C). Sirius red staining was also performed for both these populations of EHBD, demonstrating decreased fibrosis in *Prom1*^{KO} as compared with *Prom1*$^{Cre/+}$ (*Prom1*-expressing) PBGs (Figure 4D, E and Supplemental Figure 1, http://links.lww.com/HC9/A45).

In normal human EHBD, we observed expression of PROM1 and SOX9 in PBGs both proximally at the portal plate; neither was observed in the biliary epithelial lining of the lumen of the EHBD (Figure 5). In human BA samples taken at time of a Kasai portoenterostomy, which represents a later stage of BA pathogenesis, we observed PROM1 and SOX9 expression in biliary structures at the portal plate but none in the distal biliary remnant. Only 1 out of 3 biliary remnant samples displayed any residual biliary epithelium with associated PBGs; no Prom1 expression was observed in any of the biliary remnant samples.

Collectively, these results are consistent with *Prom1*-expressing progenitor cells in PBGs supporting the

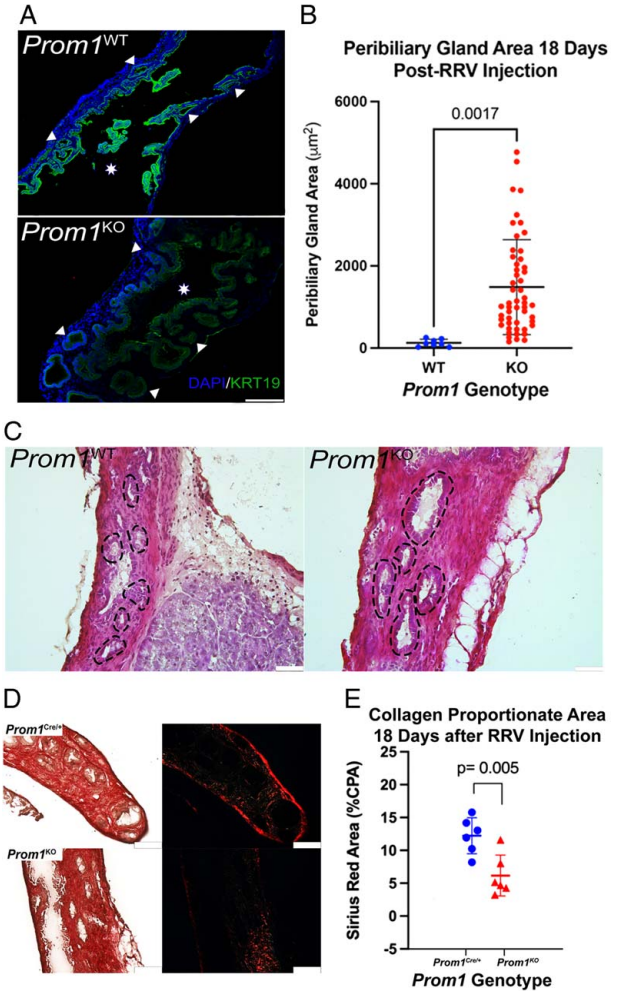

FIGURE 4 *Prom1* null mutation results in dilated PBGs 18 days after RRV injury compared with *Prom1*-expressing PBGs. (A) Mice homozygous for the *Prom*$^{Cre/Cre}$ allele were bred, resulting in functional *Prom1* knockout (*Prom1*^{KO}) mice. (A) Fluorescence imaging of KRT19 expression in both WT and *Prom1*^{KO} EHBD. Triangles point to PBGs, and stars signify EHBD lumen. Scale bar, 250 μm. (B) PBGs in *Prom1*^{KO} are larger than WT (n = 3 biological replicates). (C) Hematoxylin and eosin staining of PBGs in the EHBD demonstrates enlarged PBGs in *Prom1*^{KO} as compared with *Prom1*^{WT}. PBGs are outlined with dashed lines. Scale bars, 50 μm. (D) Sirius red staining of EHBD from *Prom1*-expressing (*Prom1*$^{Cre/+}$) and *Prom1*^{KO} 18 days after RRV injury. Scale bar, 100 μm. (E) *Prom1*-expressing EHBD (*Prom1*$^{Cre/+}$) CPA is statistically significantly higher than *Prom1*^{KO} EHBD ($p < 0.005$). Abbreviations: CPA, collagen proportionate area; EHBD, extrahepatic bile duct; PBG, peribiliary gland; *Prom1*, Prominin-1; RRV, rhesus rotavirus; WT, wild-type.

maintenance of the EHBD surface epithelium and restitution of the EHBD surface epithelium after injury.

EHBD-derived organoids are PROM1$^+$/SOX9$^+$/KRT19$^+$ and are derived from *Prom1*-expressing biliary progenitor cells residing in PBGs

We next sought to further explore the *in vivo* observation of dilated PBGs in *Prom1*^{KO} mouse pups compared with *Prom1*^{WT} following RRV injection using EHBD-derived biliary organoids *in vitro*. Organoids from the EHBD of *Prom1*^{WT} and *Prom1*^{KO} mice were grown in Matrigel, cleared, and then imaged via confocal microscopy. EHBD-derived organoids robustly express KRT19 (Supplemental Video 3). *Prom1*^{WT} organoids express PROM1 on the luminal surface of the organoid, similar to what is observed in PBGs *in vivo*, whereas PROM1 expression is absent in *Prom1*^{KO} organoids (Figure 6A). In addition to KRT19, both *Prom1*^{WT} and *Prom1*^{KO} organoids express biliary progenitor nuclear transcription factor SOX9 (Figure 6A).

Next, intact EHBD epithelium were carefully dissected from *Prom1*$^{Cre/+}$-*GFP*$^{+/-}$ mice and placed into Matrigel 1 week after *in vivo* tamoxifen injection. Sequential fluorescence images demonstrated GFP$^+$ PBGs which were observed enlarging and then budding off the EHBD (Figure 6B). We observed fewer PBG attached to EHBDs epithelium over time. These findings suggest that likely some of the cultured organoids arise from enlarging, budding PBGs populated with *Prom1*-expressing progenitor cells and their progeny.

Next, we generated EHBD biliary organoids from transgenic heterozygous *Prom1*$^{Cre/+}$-*mTmG*$^{+/-}$ mice, wherein by default, all cells express TOMATO except for *Prom1*-expressing cells and their lineage, which express GFP following tamoxifen injection. At day 2 of culture, we observed mostly GFP expression and rare TOMATO expression within organoids. At day 6, all organoids were universally GFP$^+$ with no TOMATO expression (Figure 6C), suggesting a survival advantage for organoids are derived from *Prom1*-expressing cells from PBG.

Like organoids from *Prom1*$^{+/-}$ mice, EHBD-derived organoids from *Prom1*^{KO} mice (*Prom1*$^{Cre/Cre}$-*GFP*$^{+/-}$) were also found to be entirely GFP$^+$ suggesting that EHBD-derived organoids derive from biliary progenitor cells independent of *Prom1* expression (Figure 6D). Of note, organoids grown from the biliary remnant of an infant with BA collected at the time of a Kasai portoenterostomy co-expressed Prom1 and SOX9 (Figure 6E). We posit that these human biliary organoids likely also derive from Prom1-expressing biliary progenitor cells in PBGs.

Null mutation of *Prom1* leads to decreased cellular proliferation and altered organoid dynamics

We next sought to evaluate the impact of *Prom1* null mutation on EHBD-derived organoid growth and proliferation dynamics. Organoids were dissociated into single-cell suspensions and plated into Matrigel at equal concentrations. Brightfield live imaging microscopy of newly suspended cells was performed for 2 weeks to observe

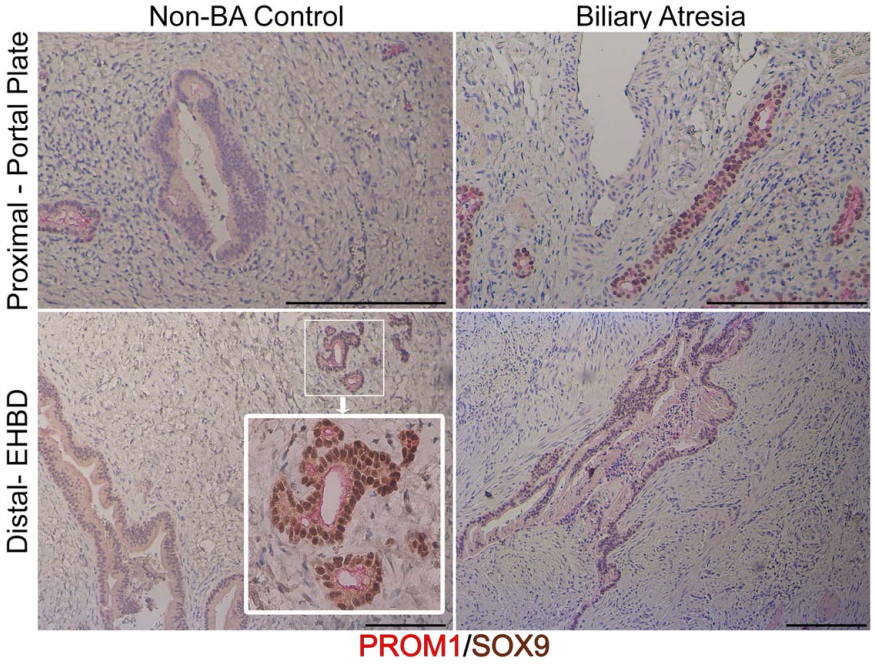

FIGURE 5 PROM1 is expressed in human peribiliary glands and in biliary epithelium of the portal plate in BA. Top panel demonstrates proximal EHBD tissue at the portal plate in non-BA control and BA sections. Immunohistochemical staining for PROM1 (red) and SOX9 (brown) reveal PROM1 expression in smaller diameter ducts in non-BA controls, which is absent in larger ducts. PROM1 and SOX9 are universally expressed in biliary tissue in BA portal plate. PROM1 is expressed in the peribiliary glands of non-BA diseased common bile duct (inset). PROM1 is not found in distal non-BA EHBD. Scale bar, 500 μm. Abbreviations: BA, biliary atresia; EHBD, extrahepatic bile duct; PROM1, Prominin-1; SOX9, sex-determining region Y-box 9.

organoid growth and behavior. Images, which were captured at 30-minute intervals, were then aligned and framed into videos (Supplemental Video 4). Individual organoids were tracked through all the frames and tracking data were then analyzed (Figure 7A). *Prom1*^{WT} organoids traveled significantly faster distances over time compared with *Prom1*^{KO} organoids (Figure 7B). *Prom1*^{WT} organoids also traveled at significantly faster rates than *Prom1*^{KO} organoids did (Figure 7C), indicating that Prom1 is important for motility.

Epithelial-derived organoids are known to exhibit oscillations in size as they grow in culture.[23] These oscillatory cycles are dependent on multiple dynamic forces such as rate of cellular proliferation, intraluminal secretion of osmotically active substrate, and surface tension. More rapid deflation-inflation size oscillations are indicative of higher levels of cellular turnover, proliferation, and organoid re-inflation. When we compared the number of size oscillation events, we observed that *Prom1*^{WT} organoids had significantly more size oscillation events per track than *Prom1*^{KO} (Figure 7D). In addition, we also found that *Prom1*^{WT} organoids grew to larger surface areas during track development than *Prom1*^{KO} (Figure 7E). Since organoids are spheres composed of a monolayer of cells, surface area is directly proportional to number of cells comprising an organoid. These observations are consistent with Prom1 supporting biliary cell proliferation.

Prom1^{KO} biliary organoids are characterized by loss of cytoskeletal polarity and altered ciliary structure

We then sought to further characterize cellular phenotypical differences between *Prom1*^{WT} and *Prom1*^{KO} biliary progenitor cells in attempts to elucidate PROM1 function in biliary progenitor cell-mediated EHBD reconstitution after injury. Given evidence that PROM1 function is involved with cytoskeletal maintenance as well as influencing cilia structure in other epithelial systems, we then investigated cellular cytoskeletal protein localization and ciliary structure in both *Prom1*-expressing and *Prom1* null mutation biliary progenitor cells. Radixin, a member of the FERM family of proteins, which anchor actin cytoskeletal fibers to the cellular plasma membrane, is known to interact with PROM1 in hepatocytes; absence of PROM1 leads to alterations in gluconeogenesis.[15] We speculated that PROM1 expression might be associated with cholangiocyte-specific FERM protein, EZRIN.[24] F-ACTIN and phosphorylated EZRIN (activated anchoring EZRIN) were evaluated via whole mount imaging of *Prom1*^{WT} versus *Prom1*^{KO} organoids. F-ACTIN and pEZRIN are both co-localized with PROM1 staining to the apical membranes of *Prom1*^{WT}; in contrast, both stain diffusely in a non-localized fashion in *Prom1*^{KO} organoids (Figure 8A, B). Abnormal polarity in *Prom1*^{KO} was further quantified with F-ACTIN apical

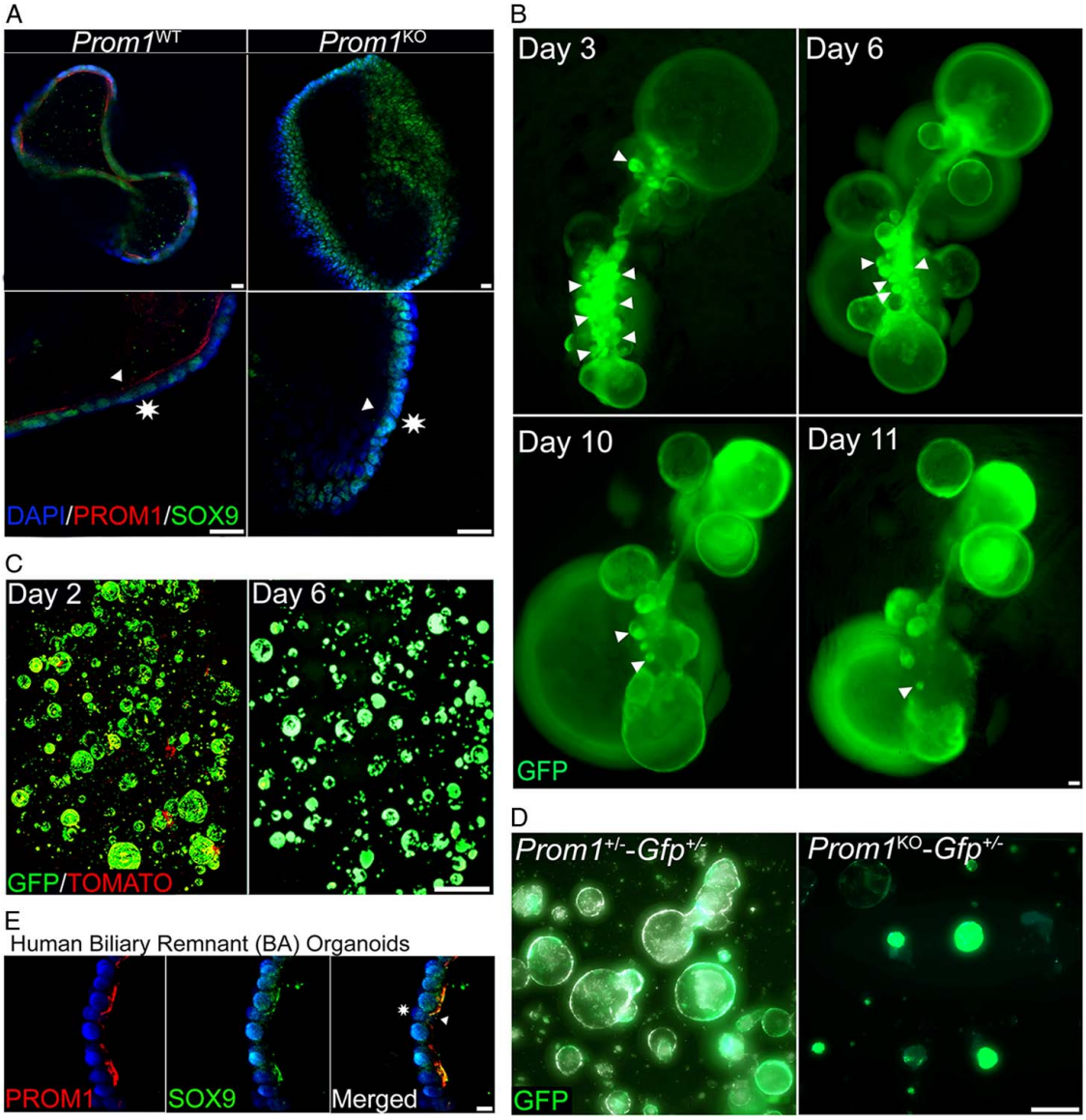

FIGURE 6 EHBD-derived organoids originate from and continue to express PROM1$^+$ PBG-residing biliary progenitor cell phenotype. (A) EHBD-derived biliary organoids universally express PROM1 (red) along the luminal surface of the organoids as well as universally express SOX9 (green). PROM1 expression is absent in *Prom1*^{KO} organoids, but SOX9 expression is maintained. Triangles point to organoid luminal surface; stars indicate basolateral surface. Scale bar, 20 μm. (B) *Prom1*$^{Cre/+}$-*GFP*$^{+/-}$ EHBD were partially digested after tamoxifen injection 1 week prior, placed in Matrigel and organoid culture media, and imaged at 5 days after culture. GFP$^+$ organoids can be seen budding from GFP$^+$ PBGs. GFP$^+$ organoids increase over time and is associated with a decreased in PBG-like structure. Triangles indicate PBGs. Scale bar, 100 μm. (C) Organoids derived from *Prom1*$^{Cre/+}$-*mTmG*$^{+/-}$ EHBDs with tamoxifen injection 1 week before EHBD dissociation display both GFP$^+$ (green) and Tomato$^+$ (red) expressing cells at 2 days of culture. Only GFP is expressed by day 6. Scale bar, 1.7 mm. (D) Organoids derived from *Prom1*$^{Cre/+}$-*GFP*$^{+/-}$ and *Prom1*$^{Cre/Cre}$-*GFP*$^{+/-}$ both express GFP. Scale bar, 200 μm. (E) Organoids derived from a biliary remnant of a patient with Biliary Atresia at time of Kasai were found to be PROM1$^+$/SOX9$^+$. Scale bar, 10 μm. Abbreviations: EHBD, extrahepatic bile duct; GFP, green fluorescent protein; PBG, peribiliary gland; PROM1, Prominin-1; SOX9, sex-determining region Y-box 9.

localization (87 ± 8.9% cells with F-ACTIN localization vs. 15.63 ± 7.8% cells, $p = 0.008$) (Figure 8E and Supplemental Video 5).

Similarly, cystic fibrosis transmembrane conductance regulator (CFTR) was co-stained with PROM1 to further investigate altered cellular polarity in *Prom1*^{KO} organoids. CFTR also co-localized with PROM1 to the apical membrane, whereas CFTR was expressed in the basolateral and apical membranes of *Prom1*^{KO} organoids (Figure 8C). These data indicate that null mutation of *Prom1* alters cytoskeletal structure, specifically cellular polarity.

Given the role of Prom1 in ciliary dynamics in other epithelial progenitor systems and observations of BA-associated ciliopathy, we assessed ciliary structure in *Prom1*^{WT} and *Prom1*^{KO} by acetylated-α-TUBULIN staining (Figure 8D).[25] Cilia in *Prom1*^{KO} organoids were less abundant (1.07 ± 0.23 vs. 0.39 ± 0.21 cilia/

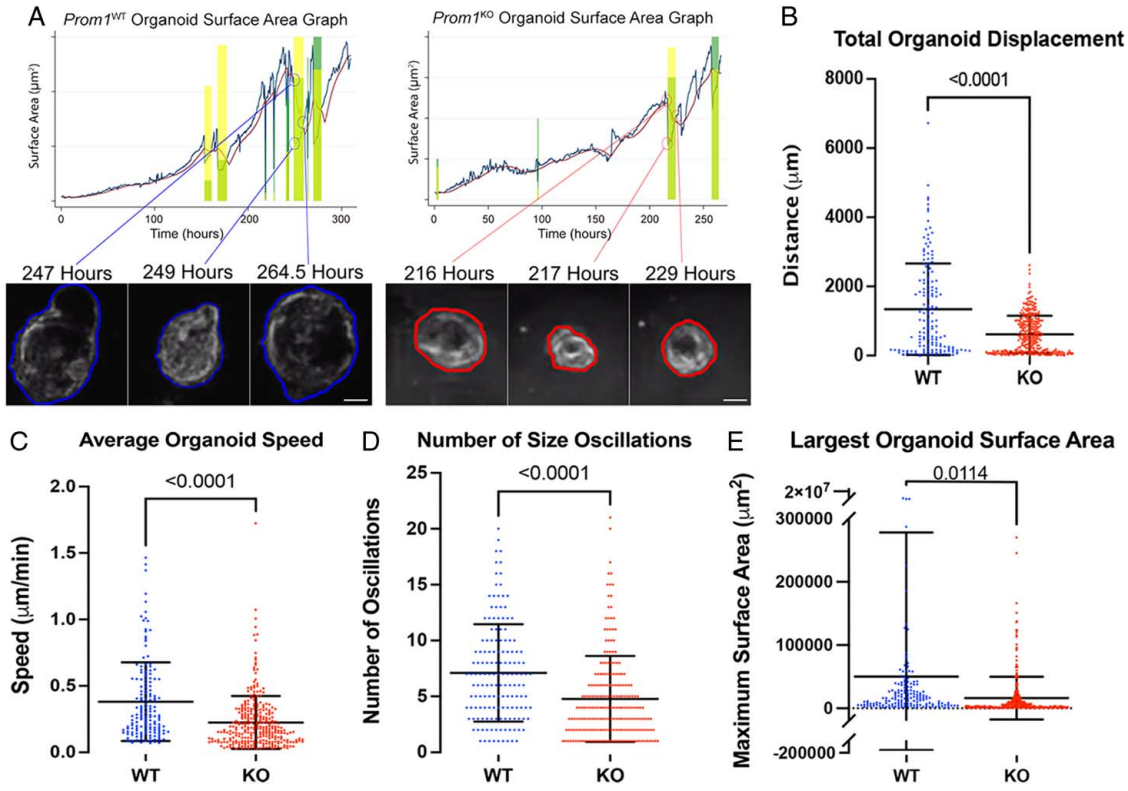

FIGURE 7 Null mutation of *Prom1* results in decreased organoid motility and growth dynamics. (A) Both *Prom1*^{WT} and *Prom1*^{KO} organoids were grown in culture and live imagined for 14 days. Time-lapse videos were made, and organoids were tracked with through time. Organoid track surface area was then graphed over time (blue line) and compared with a normalized surface area line (red line). Size oscillations were recorded (green rectangles). Organoid size oscillation examples are demonstrated in both *Prom1*^{WT} and *Prom1*^{KO} organoid tracks. Scale bar, 100 µm. Images of organoids are high-resolution and zoomed-in stills from Supplemental Video 4. (B) *Prom1*^{WT} organoids traveled nearly twice as far from their starting positions as compared with *Prom1*^{KO}. (C) *Prom1*^{WT} organoids also traveled at faster speeds than *Prom1*^{KO}. (D) *Prom1*^{WT} organoids oscillated more per track than *Prom1*^{KO}. (E) *Prom1*^{WT} organoids grew to larger surface areas during track development than *Prom1*^{KO}.

nuclei, $p = 0.02$) (Figure 8G) and smaller (1.26 ± 0.08 vs. 0.78 ± 0.23 µm, $p = 0.03$) compared with those in *Prom1*^{WT} organoids (Figure 8F and Supplemental Video 6), indicating altered biliary epithelial ciliary structure with *Prom1* null mutation.

Given the differences in both organoid behavior and cytoskeletal phenotype, we then investigated gene expression differences between *Prom1*^{WT} and *Prom1*^{KO} organoids through bulk RNA-sequencing to decipher signaling pathways that are involved in *Prom1*-related function (Supplemental Figure 2, http://links.lww.com/HC9/A46). Gene Ontology (GO) pathway analysis revealed that the top biological processes that were represented in the differentially expressed genes were related to cellular growth and cytoskeletal structure. Cilia and cytoskeletal structure and function represented 6 out of the top 16 pathways represented. Proliferative pathways including Wnt signaling were also highly represented in the differentially expressed genes (Figure 8H). Wnt11 had the largest fold expression difference in *Prom1*^{KO} as compared with *Prom1*^{WT} of all Wnt ligands. Wnt11 has been proposed as an antagonist of Wnt canonical pathways, thus possibly decreasing canonical Wnt signaling in *Prom1*^{KO} organoids.[26] This gene expression data, in parallel with organoid whole mount staining, demonstrate possible PROM1-mediated cellular mechanisms of biliary epithelial homeostasis maintenance in the EHBD.

Alterations in cellular cytoskeletal structure as displayed by altered cellular polarity and ciliary frequency and size implicates these as possible mechanisms by which *Prom1* null mutation leads to the altered phenotypes seen *in vivo* and *in vitro*.

DISCUSSION

In this study, we demonstrate that Prom1-expressing biliary progenitor cells residing in PBGs of the EHBD participate in the baseline physiological maintenance of the biliary epithelium. Proliferation of this progenitor cell population increases to support biliary epithelial restitution in response to injury. Null mutation of *Prom1* results in an altered phenotype of dilated PBGs *in vivo*, decreased *Prom1*-expressing PBG progenitor cell contribution to EHBD luminal epithelium after injury, as well as less motile, less dynamic, and less proliferative organoids. Loss

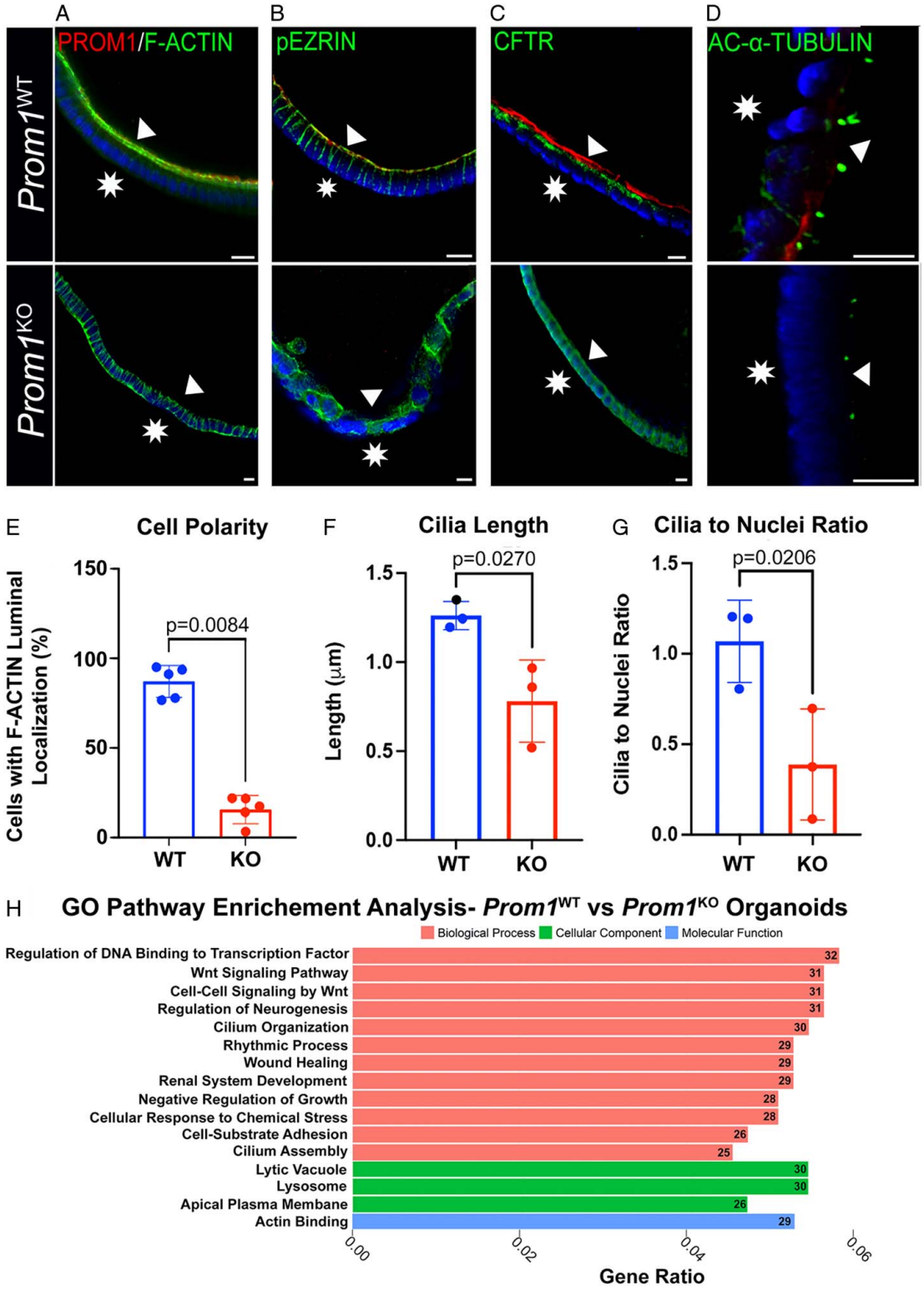

FIGURE 8 *Prom1* null mutation is associated with absent cellular polarity and abnormal ciliary structure in biliary organoids. (A–D) Cytoskeletal proteins F-ACTIN, phosphorylated EZRIN (pEZRIN), and cystic fibrosis transmembrane conductance regulator (CFTR) are localized to the apical membrane in WT organoids but are diffusely expressed in *Prom1*^{KO} organoids. Cilia protein acetylated (AC)-α-tubulin staining demonstrates altered cilia structure in *Prom1*^{KO} organoids. Triangles point to the luminal membrane and stars signify the basolateral organoid membrane. Scale bars, 10 μm. (E) There is a higher percentage of diffusely staining F-ACTIN cells in KO versus WT organoids (n = 3 biological replicates). Cilia are longer (F) and denser (G) in *Prom1*^{WT} versus *Prom1*^{KO} (n = 3 biological replicates). (H) Gene Ontology (GO) pathway analysis of DEGs from RNA-sequencing of *Prom1*^{WT} organoids as compared with *Prom1*^{KO} organoids. Numbers at end of bars represent number of differentially expressed genes in a pathway represented.

of *Prom1* leads to altered ciliary structure and cellular polarity in organoids, similar to phenotypical changes seen in the biliary epithelium seen in cholestatic disease states (Supplemental Figure 3, http://links.lww.com/HC9/A47).

Both cellular polarity and cilia influence stem/progenitor cell motility and proliferation.[27–31] Cilia are integral for cellular sensory of environmental stimuli and subsequent proliferative downstream signaling pathways such as Wnt in response to stimuli.[32] In addition, primary cilia and cell polarity are both pathways implicated in epithelial cellular migration.[33,34] In fact, the chemosensory properties of primary cilia were implicated in cholangiocyte migration and invasion in a cholangiocarcinoma *in vitro* model.[31] In this study, we have demonstrated that altered cellular polarity and cilia in *Prom1*^{KO} organoids are associated with decreased organoid motility and proliferation. We posit that altered cellular motility and proliferative dynamics on an organized multicellular level, as exemplified by the *Prom1*^{KO} organoid observations, could be representative of impaired migratory capacity of PBG progenitor cell lineage into the EHBD lumen, as exemplified by decreased luminal epithelial lineage in *Prom1*^{KO} mice after injury, and subsequent PBG dilation. This may be phenotypically apparent when rapid proliferation of the EHBD surface epithelium is required, such as in injury states or during organ development. These are both processes in which we have demonstrated that *Prom1*-expressing cell lineage reconstitute the EHBD epithelium in both adult and neonatal murine EHBDs. Dysfunction of this physiological process may contribute to the PBG dilation that was demonstrated after RRV injury in *Prom1*^{KO} EHBD. Defects in the ability of biliary progenitor cells to re-populate the EHBD lumen may also contribute to cholestatic biliary pathology as exemplified by the absence of Prom1 expression in the distal EHBD of BA patients, with prevalent Prom1 expression of biliary epithelium in BA portal plate sections. Failure of biliary progenitor cells to reconstitute the EHBD lumen may be present in combination with other leading models of EHBD injury in cholangiopathies such as BA.

A recent genome-wide association studies of BA patients detected Prom1 missense mutations in the BA cohort.[16] While complete null mutation of *Prom1* in RRV-mediate BA is not associated with greater magnitude of EHBD obliteration, it is associated with a reduction in intrahepatic ductular reactions and fibrosis.[3] It is possible that these missense mutations in *Prom1* are associated with alterations in Prom1 function but not complete loss of function.

Abnormal biliary epithelial cilia have been demonstrated in cholangiopathies as well. Histology of EHBD from BA patients exhibit absence of cilia in the surface epithelium but not within the PBGs.[35] BA has been associated with polymorphisms of structural proteins such as Adducin-3, a known actin-binding cytoskeletal scaffolding protein, and PKD1L1, a protein known to be essential for ciliary movement.[36] Associations of biliary ciliary dysfunction and liver disease are also seen in polycystic liver disease in conjugation or separate from autosomal dominant and recessive polycystic kidney diseases.[37] Primary sclerosing cholangitis is associated with elongated cilium as compared with normal control cholangiocytes.[38] Biliary epithelial proliferation in cholangiocarcinoma models has been shown to be dependent on cholangiocyte ciliary function, further linking ciliary structure and function with biliary epithelial proliferation.[39] The loss of ciliary length and density associated with null mutation of *Prom1* provides insight into the potential role Prom1 may play in cholangiopathies.

In conclusion, *Prom1*-expressing population of biliary progenitor cells residing in PBGs participate in the normal physiological turnover of EHBD luminal epithelium and biliary epithelial restitution during injury. Null mutation of *Prom1* is associated with dilated PBGs potentially due to impaired progenitor cell polarization and decreased cell migratory potential. *Prom1* acts to regulate biliary cytoskeletal polarity as well as ciliary dynamics in biliary progenitor proliferation. Further characterization of Prom1-expressing progenitor cells in biliary development and in response to injury may provide new insights into the pathogenesis of cholangiopathies and epithelial biology.

AUTHOR CONTRIBUTIONS

A.Z., K.A., and K.W. helped in conception and design of research. A.Z., C.S., J.X., N. Malkoff, N.N., E.F., A.G., and T.Y. performed experiments. A.Z. analyzed data. A.Z., C.S., J.X., N. Mavila, K.A., and K.W. interpreted results of experiments. A.Z., C.S., and K.W. prepared figures. A.Z., C.S., N. Mavila, K.A., and K.W. drafted manuscript.

CONFLICTS OF INTEREST

Nothing to report.

ORCID

Allen Zhong https://orcid.org/0000–0002–8102–6696
Celia Short https://orcid.org/0000–0002–4457–0123
Jiabo Xu https://orcid.org/0000–0002–2314–8089
G. Esteban Fernandez https://orcid.org/0000–0002–8393–9229
Nicolas Malkoff https://orcid.org/0000–0002–3519–6790
Nicolas Noriega https://orcid.org/0000–0001–6573–1611
Theresa Yeo https://orcid.org/0000–0003–0760–933X
Larry Wang https://orcid.org/0000–0002–5275–3165
Nirmala Mavila https://orcid.org/0000–0002–5608–3349
Kinji Asahina https://orcid.org/0000–0003–0398–8395
Kasper S. Wang https://orcid.org/0000–0003–0487–6416

REFERENCES

1. Zagory JA, Nguyen MV, Wang KS. Recent advances in the pathogenesis and management of biliary atresia. Curr Opin Pediatr. 2015;27:389–94.
2. Moreira RK, Cabral R, Cowles RA, Lobritto SJ. Biliary atresia: a multidisciplinary approach to diagnosis and management. Arch Pathol Lab Med. 2012;136:746–60.

3. Zagory JA, Fenlon M, Dietz W, Zhao M, Nguyen MV, Trinh P, Adoumie M, et al. Prominin-1 promotes biliary fibrosis associated with biliary atresia. Hepatology. 2019;69:2586–97.
4. Fenlon M, Short C, Xu J, Malkoff N, Mahdi E, Hough M, Glazier A, et al. Prominin-1-expressing hepatic progenitor cells induce fibrogenesis in murine cholestatic liver injury. Physiol Rep. 2020; 8:e14508.
5. Nguyen MV, Zagory JA, Dietz WH, Park A, Fenlon M, Zhao M, Xu J, et al. Hepatic prominin-1 expression is associated with biliary fibrosis. Surgery. 2017;161:1266–72.
6. Kamimoto K, Kaneko K, Kok CY, Okada H, Miyajima A, Itoh T. Heterogeneity and stochastic growth regulation of biliary epithelial cells dictate dynamic epithelial tissue remodeling. eLife. 2016;5:e15034.
7. Zhu L, Finkelstein D, Gao C, Shi L, Wang Y, López-Terrada D, Wang K, et al. Multi-organ mapping of cancer risk. Cell. 2016; 166:1132–146.e7.
8. Liou GY. CD133 as a regulator of cancer metastasis through the cancer stem cells. Int J Biochem Cell Biol. 2019;106:1–7.
9. Singer D, Thamm K, Zhuang H, Karbanová J, Gao Y, Walker JV, Jin H, et al. Prominin-1 controls stem cell activation by orchestrating ciliary dynamics. EMBO J. 2019;38:e99845.
10. Barzegar Behrooz A, Syahir A, Ahmad S. CD133: beyond a cancer stem cell biomarker. J Drug Target. 2019;27:257–69.
11. Snippert HJ, van Es JH, van den Born M, Begthel H, Stange DE, Barker N, Clevers H. Prominin-1/CD133 marks stem cells and early progenitors in mouse small intestine. Gastroenterology. 2009;136:2187–194.e1.
12. Wang H, Gong P, Li J, Fu Y, Zhou Z, Liu L. Role of CD133 in human embryonic stem cell proliferation and teratoma formation. Stem Cell Res Ther. 2020;11:208.
13. Charruyer A, Strachan LR, Yue L, Toth AS, Cecchini G, Mancianti ML, Ghadially R. CD133 is a marker for long-term repopulating murine epidermal stem cells. J Invest Dermatol. 2012;132:2522–33.
14. Jaszai J, Thamm K, Karbanova J, Janich P, Fargeas CA, Huttner WB, Corbeil D. Prominins control ciliary length throughout the animal kingdom: new lessons from human prominin-1 and zebrafish prominin-3. J Biol Chem. 2020;295:6007–22.
15. Lee H, Yu DM, Park JS, Kim JS, Kim HL, Koo SH, Lee JS, et al. Prominin-1-Radixin axis controls hepatic gluconeogenesis by regulating PKA activity. EMBO Rep. 2020;21:e49416.
16. Lam WY, Tang CS, So MT, Yue H, Hsu JS, Chung PH, Nicholls JM, et al. Identification of a wide spectrum of ciliary gene mutations in nonsyndromic biliary atresia patients implicates ciliary dysfunction as a novel disease mechanism. EBioMedicine. 2021;71:103530.
17. DiPaola F, Shivakumar P, Pfister J, Walters S, Sabla G, Bezerra JA. Identification of intramural epithelial networks linked to peribiliary glands that express progenitor cell markers and proliferate after injury in mice. Hepatology. 2013;58:1486–96.
18. Carpino G, Nevi L, Overi D, Cardinale V, Lu WY, Di Matteo S, Safarikia S, et al. Peribiliary gland niche participates in biliary tree regeneration in mouse and in human primary sclerosing cholangitis. Hepatology. 2020;71:972–89.
19. Krüger I, Reusswig F, Krott KJ, Lersch CF, Spelleken M, Elvers M. Genetic labeling of cells allows identification and tracking of transgenic platelets in mice. Int J Mol Sci. 2021;22:3710.
20. Mohanty SK, Donnelly B, Temple H, Tiao GM. A rotavirus-induced mouse model to study biliary atresia and neonatal cholestasis. Methods Mol Biol. 2019;1981:259–71.
21. Mariotti V, Strazzabosco M, Fabris L, Calvisi DF. Animal models of biliary injury and altered bile acid metabolism. Biochim Biophys Acta Mol Basis Dis. 2018;1864:1254–61.
22. Mohanty SK, Donnelly B, Bondoc A, Jafri M, Walther A, Coots A, McNeal M, et al. Rotavirus replication in the cholangiocyte mediates the temporal dependence of murine biliary atresia. PLoS One. 2013;8:e69069.
23. Hof L, Moreth T, Koch M, Liebisch T, Kurtz M, Tarnick J, Lissek SM, et al. Long-term live imaging and multiscale analysis identify heterogeneity and core principles of epithelial organoid morphogenesis. BMC Biol. 2021;19:37.
24. Fouassier L, Fiorotto R. Ezrin finds its groove in cholangiocytes. Hepatology. 2015;61:1467–70.
25. Chu AS, Russo PA, Wells RG. Cholangiocyte cilia are abnormal in syndromic and non-syndromic biliary atresia. Mod Pathol. 2012;25:751–7.
26. Maye P, Zheng J, Li L, Wu D. Multiple mechanisms for Wnt11-mediated repression of the canonical Wnt signaling pathway. J Biol Chem. 2004;279:24659–65.
27. Halaoui R, McCaffrey L. Rewiring cell polarity signaling in cancer. Oncogene. 2015;34:939–50.
28. Zeitler J, Hsu CP, Dionne H, Bilder D. Domains controlling cell polarity and proliferation in the *Drosophila* tumor suppressor Scribble. J Cell Biol. 2004;167:1137–46.
29. Nabi IR. The polarization of the motile cell. J Cell Sci. 1999;112 (pt 12):1803–11.
30. Masyuk AI, Huang BQ, Ward CJ, Gradilone SA, Banales JM, Masyuk TV, Radtke B, et al. Biliary exosomes influence cholangiocyte regulatory mechanisms and proliferation through interaction with primary cilia. Am J Physiol Gastrointest Liver Physiol. 2010;299:G990–9.
31. Mansini AP, Peixoto E, Thelen KM, Gaspari C, Jin S, Gradilone SA. The cholangiocyte primary cilium in health and disease. Biochim Biophys Acta Mol Basis Dis. 2018;1864:1245–53.
32. Waters AM, Beales PL. Ciliopathies: an expanding disease spectrum. Pediatr Nephrol. 2011;26:1039–56.
33. Diaz R, Kronenberg NM, Martinelli A, Liehm P, Riches AC, Gather MC, Paracchini S. KIAA0319 influences cilia length, cell migration and mechanical cell-substrate interaction. Sci Rep. 2022;12:722.
34. Campanale JP, Sun TY, Montell DJ. Development and dynamics of cell polarity at a glance. J Cell Sci. 2017;130:1201–7.
35. Karjoo S, Hand NJ, Loarca L, Russo PA, Friedman JR, Wells RG. Extrahepatic cholangiocyte cilia are abnormal in biliary atresia. J Pediatr Gastroenterol Nutr. 2013;57:96–101.
36. Berauer JP, Mezina AI, Okou DT, Sabo A, Muzny DM, Gibbs RA, Hegde MR, et al. Identification of polycystic kidney disease 1 like 1 gene variants in children with biliary atresia splenic malformation syndrome. Hepatology. 2019;70:899–910.
37. Larusso NF, Masyuk TV. The role of cilia in the regulation of bile flow. Dig Dis. 2011;29:6–12.
38. Masyuk TV, Masyuk AI, LaRusso NF. TGR5 in the cholangiociliopathies. Dig Dis. 2015;33:420–5.
39. Mansini AP, Peixoto E, Jin S, Richard S, Gradilone SA. The chemosensory function of primary cilia regulates cholangiocyte migration, invasion, and tumor growth. Hepatology. 2019;69: 1582–98.

How to cite this article: Zhong A, Short C, Xu J, Fernandez GE, Malkoff N, Noriega N, et al. Prominin-1 promotes restitution of the murineMAQ: Editorial Office/AASLD: Please indicate if a visual abstract will be forthcoming for this article. extrahepatic biliary luminal epithelium following cholestatic liver injury. Hepatol Commun. 2023;7:e0018. https://doi.org/10.1097/HC9.0000000000000018